Radiology Case Reports 17 (2022) 4859–4867

Available online at www.sciencedirect.com

ScienceDirect

journal homepage: www.elsevier.com/locate/radcr

Case Report

Erdheim-Chester disease: Typical radiologic findings of a multisystemic disease ☆

André Peixoto, MD[a,*], *Guilherme Martins, MD*[b], *João Leitão, MD*[a]

[a] *Serviço de Imagiologia Geral, Centro Hospitalar Universitário Lisboa Norte, Av. Prof. Egas Moniz, Lisboa 1649-035, Portugal*

[b] *Serviço de Imagiologia Neurológica, Centro Hospitalar Universitário Lisboa Norte, Lisboa 1649-035, Portugal*

ARTICLE INFO

Article history:
Received 10 August 2022
Revised 23 August 2022
Accepted 25 August 2022

Keywords:
Erdheim-Chester disease
Bone pain
Diabetes insipidus
Hairy kidney
Coated aorta
Right atrium pseudotumor
Periorbital masses

ABSTRACT

Erdheim-Chester disease is a rare and multisystemic entity. It results from the infiltration of tissues by foamy histiocytes. The etiology is unknown, but there are mutations in the MAPK pathway in over 80% of patients, more frequently BRAF mutation. The most commonly affected organs and systems are the skeleton, central nervous system, cardiovascular system, kidney, lungs, and skin. The most common clinical manifestations are bone pain, usually in the lower limbs, and diabetes insipidus. The diagnosis is challenging. It requires a combination of clinical, radiological, histopathological, and molecular findings. We present the case of a patient with typical clinical and radiological manifestations: bone pain and diabetes insipidus at presentation, bilateral long bone cortical sclerosis, hairy kidney appearance, coated aorta, right atrium pseudotumor, and periorbital masses.

Introduction

Erdheim-Chester disease (ECD) is a rare entity. It results from the infiltration of tissues by foamy cells histiocytes. Awareness of this disease has increased the number of patients diagnosed with it in recent years [1].

ECD usually affects adults in the fifth to seventh decades of life. In some cohorts, there is a male preponderance, while some authors suggest it affects males and females equally [2,3].

The etiology of ECD is unknown. However, there is evidence of mutations activating the MAPK pathway in over 80% of patients, at least half of them being the BRAFV600E activating mutation. There is an overlap with Langerhans cells histiocytosis in 15% of patients and coexist myeloproliferative neoplasms or myelodysplastic syndromes in 10% of patients [1,2,4].

☆ Competing Interests: The author declares that he has no known competing financial interests or personal relationships that could have appeared to influence the work reported in this paper.

* Corresponding author.
E-mail address: av_b14@hotmail.com (A. Peixoto).

https://doi.org/10.1016/j.radcr.2022.08.097

The histiocytic infiltration is usually multisystemic, resulting in systemic and local inflammation and consequent organ damage. The most commonly affected organs and systems are the bone, nervous system, endocrine glands, orbits, cardiovascular system, retroperitoneum, skin, and lungs [4,5].

ECD has many clinical manifestations: bone pain, diabetes insipidus, xanthelasmas, and exophthalmos are frequent symptoms at presentation [1,2,6].

Diagnosis is often delayed months to years after clinical presentation. It requires the conjugation of clinical, radiographic, histopathologic, and molecular features [1,5].

Some typical radiological findings include long bone bilateral cortical sclerosis, hairy kidney appearance on computed tomography scan (CT), coated aorta, and the right atrium pseudotumor [1,7,8].

On histopathology, the demonstration of xanthogranulomatous infiltrates with foamy histiocytes, $CD68^+$ or $CD136^+$ and $CD1a^-$ corroborates the diagnosis of ECD [1,5,9].

ECD entails significant morbidity and mortality. Overall, the 5-year survival of ECD is around 70%-80%. Currently, treatment includes Interferon-α, BRAF, and MEK inhibitors [5,6,10].

Case report

A 60-year-old male with no significant medical history had been admitted to the emergency room several times over 2 years, complaining of weakness, weight loss, leg pain, polydipsia, and polyuria. He underwent endocrinology and urology consultation. The cause of his symptoms was thought to be diabetes insipidus, but no definitive diagnosis was made.

The patient went to the emergency room again due to pain in the right hemithorax. He also felt pain in his left eye for several months. Physical examination only showed slight exophthalmia, and laboratory analysis showed increased inflammatory parameters (C-reactive protein and erythrocyte sedimentation rate). The patient was hospitalized for further investigation.

Kidney, liver, and thyroid function, viral serologies, autoimmunity, complement, and IgG were all normal.

Orbital CT showed a retro-orbital hypodense and infiltrative soft tissue lesion in the intraconal space (Fig. 1). In subsequent magnetic resonance imaging (MRI), the soft tissue was hypointense on T1-weighted images (T1WI) and T2-weighted images (T2WI), and had enhancement after contrast injection (Fig. 2).

Body CT demonstrated hypodense soft tissue circumferentially involving the aorta and its branches—"coated aorta sign" (Fig. 3). There were also soft tissue masses bilaterally in perirenal and posterior pararenal spaces—"hairy kidney"—as well as soft tissue extending into the renal pelvis causing moderate hydronephrosis bilaterally (Fig. 4).

There was an enhancing soft tissue mass surrounding the right atrium and in the right atrioventricular groove encasing the coronary artery (Fig. 5). Pericardial thickening and effusion were also present (Fig. 6). Cardiac MRI showed a hypointense mass with late enhancement surrounding the right atrium and the aorta (Fig. 7).

Fig. 1 – Unenhanced orbital computed tomography, axial (A) and coronal (B) images show hypodense and infiltrating soft tissue (stars) in retro-orbital, intraconal location, eccentrically displacing the extraocular muscles.

Thoracic CT showed smooth thickening of intralobular and interlobular pulmonary septa (Fig. 8).

The review of a 2-year-old leg radiograph demonstrated bilateral cortical sclerosis affecting metaphysis and diaphysis of femurs and tibias (Fig. 9).

Biopsy of skin showed infiltration by foamy histiocytes, CD68+, on histopathology evaluation.

The definitive diagnosis was ECD, and the patient began treatment with Interferon-α.

Discussion

Clinical manifestations of ECD depend on the affected system and could be indolent or life-threatening. Organ system involvement frequencies vary in different case series [3,5].

The soft-tissue infiltration is habitually hypodense on CT. On MRI, it is isointense to hypointense on both T1WI and T2WI. These lesions have mild enhancement and are hypermetabolic on 18F-FDG PET-CT [7,8].

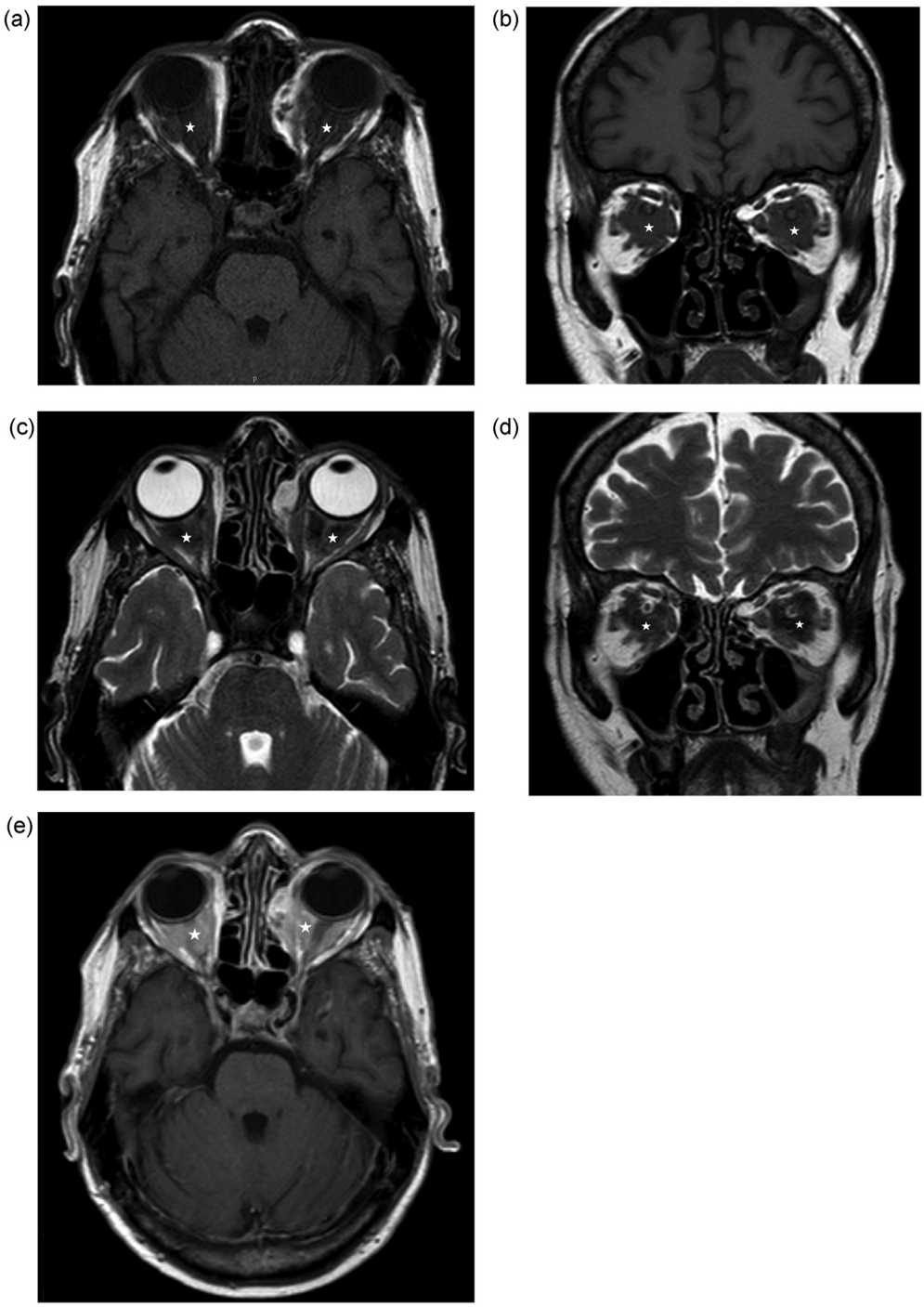

Fig. 2 – Orbital MRI, T1WI axial (A) and coronal (B), T2WI axial (C), and coronal (D) images demonstrate the soft tissue mass (stars), in intraconal location, without apparent reduction of the peri-neural subarachnoid space. It is hypointense on T1WI and T2WI. T1WI postcontrast (E) exhibits homogeneous mass enhancement.

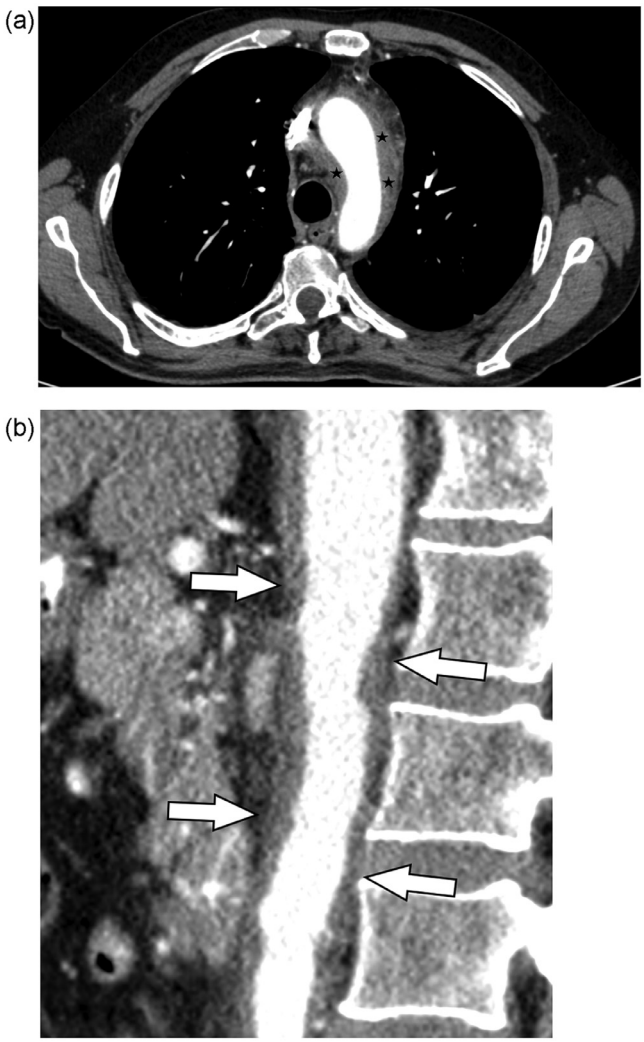

Fig. 3 – Enhanced computed tomography, axial (A) view shows soft tissue circumferentially involving the thoracic aorta (stars). The coronal (B) view demonstrates the involvement of the abdominal aorta (arrows). It is the "coated aorta sign."

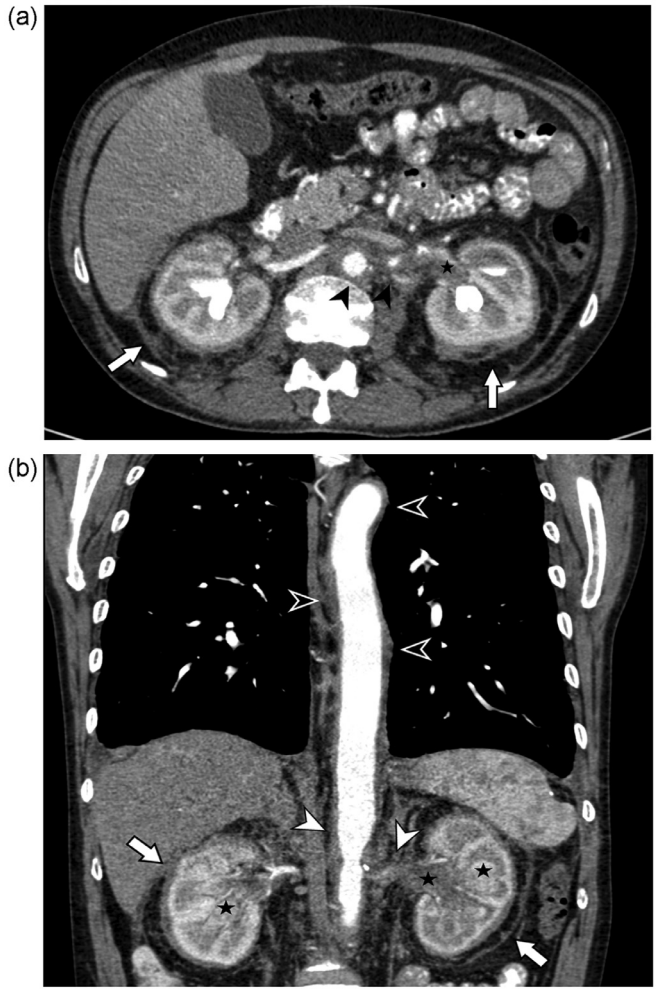

Fig. 4 – Enhanced computed tomography, axial (A), and coronal (B) views show hypodense irregular soft tissue masses in bilateral perirenal and pararenal spaces (arrows). It is the "hairy kidney." Involvement of the renal pelvis (star) is causing moderate hydronephrosis bilaterally. Corticomedullary and renal excretory phases are present because we used a split bolus technique. In these images, we can also see the circumferential involvement of the aorta and its branches (arrowheads).

Skeletal system involvement

The appendicular skeleton, particularly the long bones of the lower extremity, is involved in 74%-96% of patients. Around half of the patients present mild bone pain, frequently in the knees and ankles [3,6].

Plain radiographs display symmetrical, bilateral cortical sclerosis affecting metaphysis and diaphysis and loss of cortico-medullary differentiation of the long tubular bones [7,8,11].

99mTc bone scintigraphy and 18F-FDG PET-CT show strong bilateral and symmetric uptake in the distal ends of the long bones. These findings are a hallmark of ECD [12].

Osteosclerosis of facial or skull bones is also frequent [13].

Central nervous system involvement

About half of the cases have CNS involvement. It is a strong prognostic factor and a significant cause of mortality [1,14].

Diabetes insipidus is one of the most common manifestations, resulting from the involvement of the posterior lobe of the pituitary gland or infundibulum. On MRI, patients can have a normal hypothalamic-pituitary axis, thickening pituitary stalk, or FLAIR hyperintensity within the hypothalamus [6,15].

Neurologic symptoms include imbalance, headache, cognitive change, dysarthria, and diplopia [16].

Dural and meningeal may be diffusely infiltrated or may have discrete masses [8,17].

Intra-axial lesions can manifest as focal signal intensity changes or as space-occupying lesions. On MRI, the most frequent findings are T2WI hyperintense white matter changes and T2WI hyperintense lesions in the brainstem and cerebellum. The involvement of the vertebral

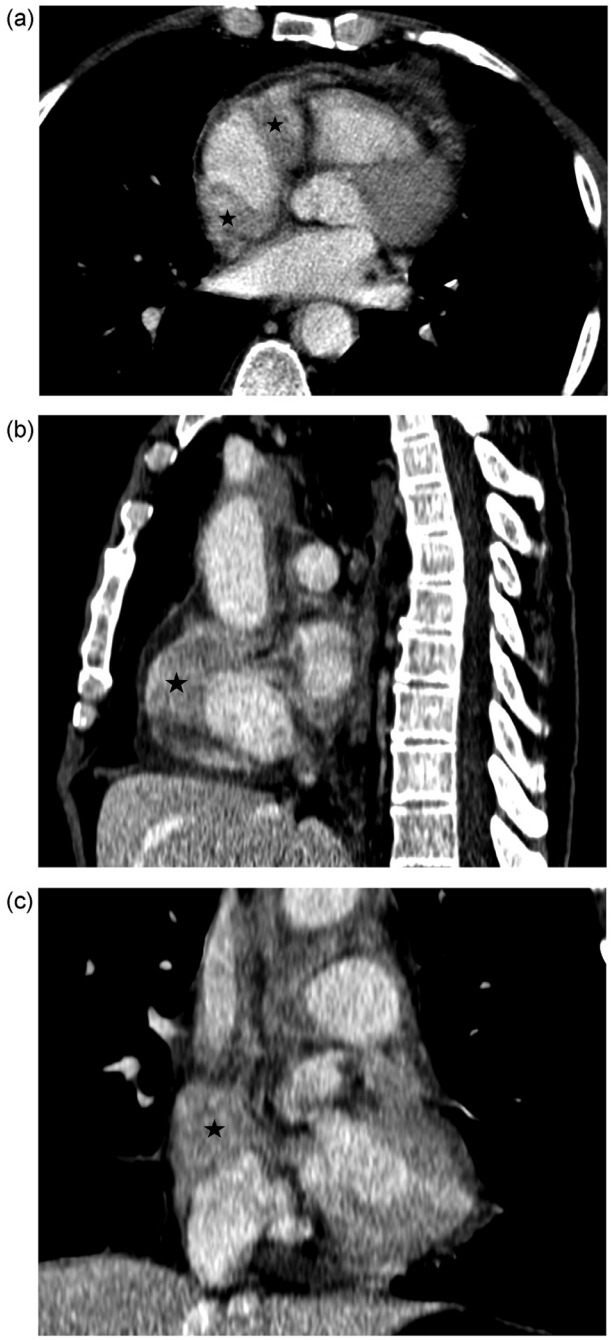

Fig. 5 – Enhanced computed tomography, axial (A), sagittal (B), and coronal (C) views demonstrate the enhancing soft tissue mass surrounding the right atrium and in the right atrioventricular (stars). It is the typical right atrium pseudotumor.

column includes enhancing lesions in the intramedullary spinal cord and T2WI hypointense epidural infiltration [17].

Orbit involvement

Orbital involvement occurs in about 25% of patients, leading to exophthalmos, which is usually bilateral and symmetrical. Lesions are habitually intraconal but can be extraconal [15,18].

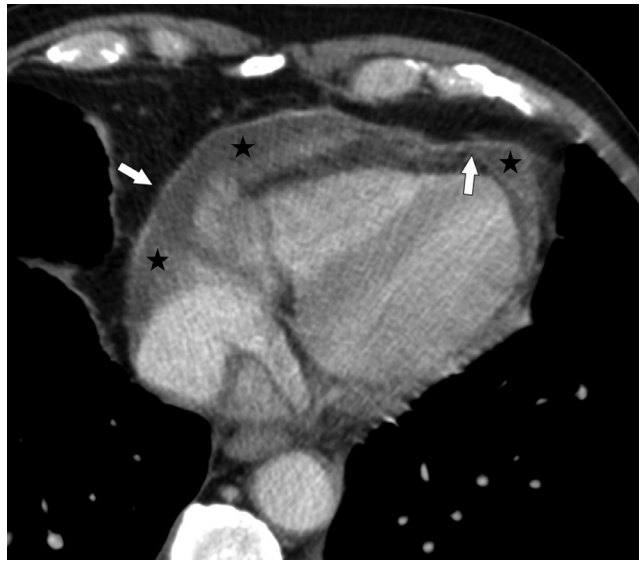

Fig. 6 – Enhanced computed tomography, axial image, demonstrates pericardial thickening (arrows) and effusion (stars).

Cardiovascular system involvement

Cardiovascular involvement is common, affecting 50%-70% of patients, but can be asymptomatic. It is a significant cause of mortality, secondary to cardiomyopathy, valve insufficiency, arrhythmias, or arterial stenosis and consequent ischemic complications [7,19].

Soft tissue infiltration encircles the aorta, the classic "coated aorta sign," and may contiguously extend along thoracic and abdominal branches. There is no associated dilation or dissection. Periarterial infiltration of coronary arteries affects 27% of patients [19,20].

Cardiac infiltration has a predilection for the right atrium and atrioventricular groove. The right atrium pseudotumor is typical [7,19].

Pericardial involvement is also frequent and manifests as thickening and effusion [19].

Renal and retroperitoneum involvement

Retroperitoneum and kidneys are involved in 65%-68% of cases [2,3].

Symmetric and bilateral irregular soft-tissue infiltration of the perirenal and posterior pararenal space forms the "hairy kidney sign." Soft tissue infiltration can involve renal sinuses and proximal ureters, causing pyelocaliceal dilatation [7,21].

Adrenal infiltration is frequent; however, adrenal insufficiency is rare [22].

Pulmonary involvement

Lung parenchyma and pleura are affected in 30%-50% of cases; however, patients usually remain asymptomatic. The most

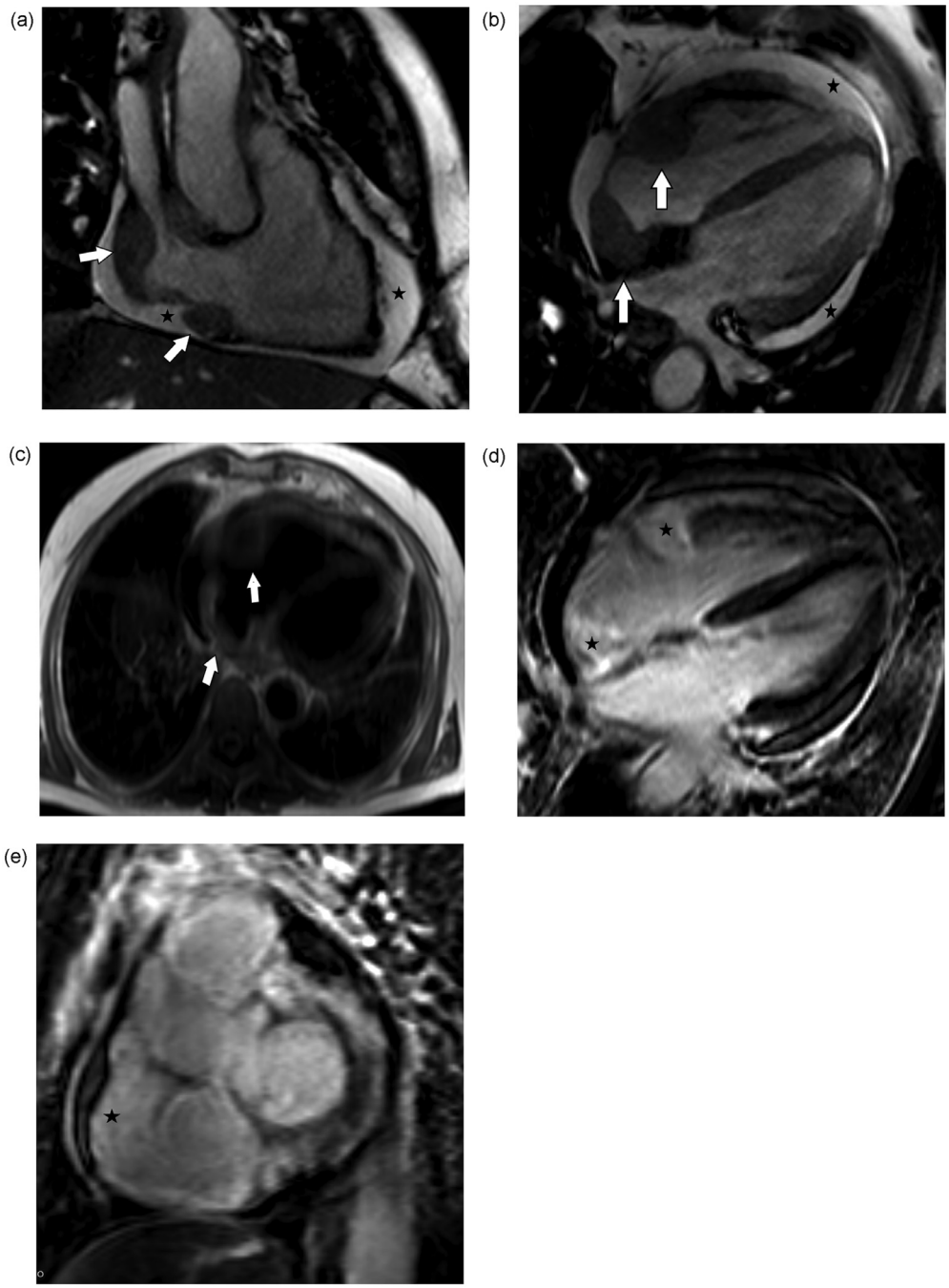

Fig. 7 – Cardiac MRI, 2-chamber (A) and 4-chamber balanced steady-state free precession (B) images show hypointense infiltration within the atrioventricular groove encircling the right coronary artery and surrounding right atrium walls (arrows). There is pericardial effusion (stars). Double inversion recovery "axial black blood" (C) image demonstrates slight hyperintensity infiltration in the right atrioventricular groove surrounding the right coronary artery, posterior right atrium wall, and interatrial septum (arrows). Postcontrast 4-chamber (D) and short axis (E) images show conspicuous late gadolinium enhancement of the infiltrating tissue (stars).

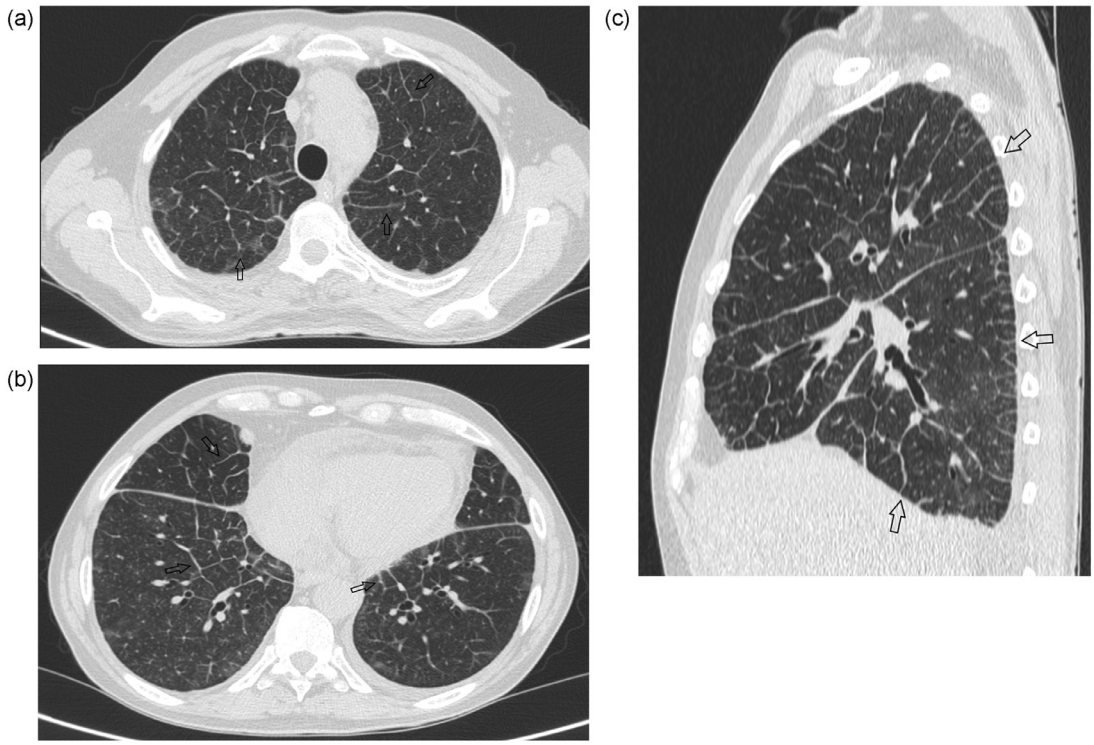

Fig. 8 – Chest computed tomography of upper lobes (A) and lower lobes (B) on axial and sagittal (C) views show smooth thickening of interlobular pulmonary septa (arrows).

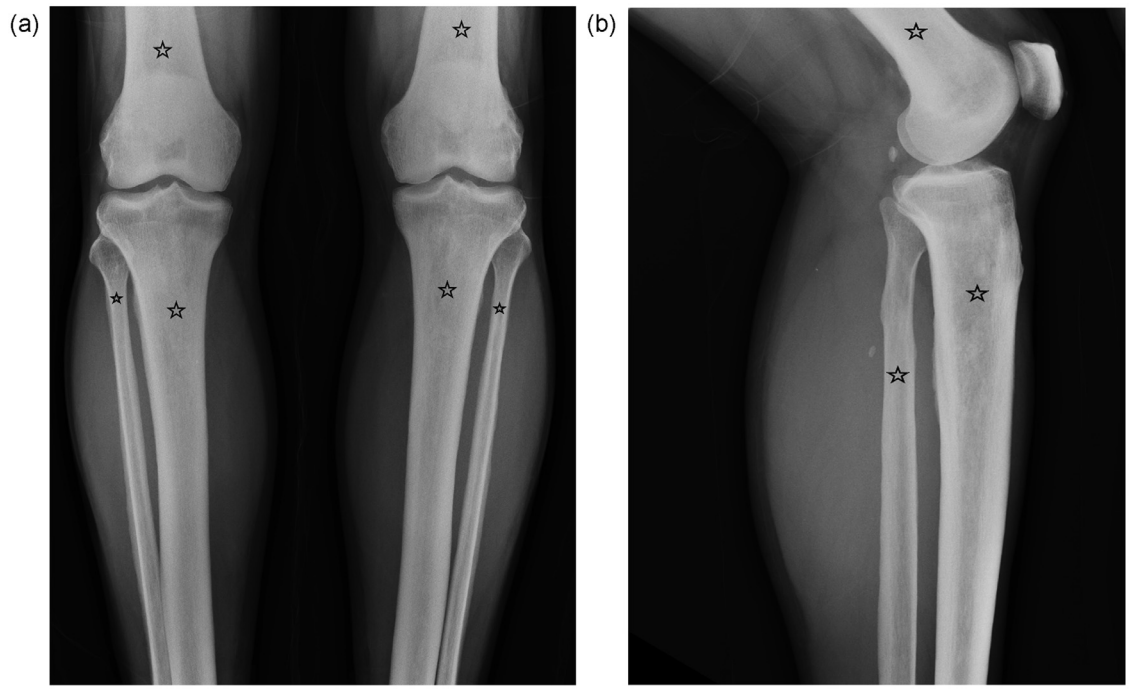

Fig. 9 – Leg radiograph, frontal (A) and lateral (B) views exhibiting the bilateral cortical sclerosis and loss of cortico-medullary differentiation (stars), affecting metaphysis and diaphysis of femurs, tibias, and fibulas.

frequent finding on CT is an interstitial lung disease-like pattern with smooth interlobular septal thickening. Centrilobular micronodular opacities and ground glass opacities are other observable features. Consolidations and cysts are infrequent. Pleural involvement is more common on the right side and presents as pleural thickening and effusion [23].

Differential diagnosis includes Langerhans cell histiocytosis, immunoglobulin G4 (IgG4)-related disease, Paget's disease, Graves' disease, retroperitoneal fibrosis, and Takayasu arteritis. However, the combination of features affecting various systems, as presented in our case, is characteristic of ECD [1,7].

Imaging exams are also essential in the follow-up. 18F-FDG PET-CT is considered the best modality for ECD response assessment and should be performed 3-6 months after initiation of therapy. CT or MRI of specific systems affected, such as the heart, brain, or orbit, could be obtained 3-6 months after diagnosis and every 6-12 months if the disease stabilizes. Treated lesions may not fully regress; however, this may not reflect the disease's activity [5,12,24].

Conclusion

The typical ECD radiological manifestations are long bone bilateral cortical sclerosis, periorbital masses, hairy kidney appearance, coated aorta, and the right atrium pseudotumor. Diagnosis of this disease is often delayed months to years. Therefore, radiologists must recognize these characteristic features of ECD.

Ethics

There are no ethical issues for the publication of this case report according to the standard of our institution.

Patient consent

The patient's informed consent for the publication of this case was granted.

REFERENCES

[1] Haroche J, Cohen-Aubart F, Amoura Z. Erdheim-Chester disease. Blood 2020;135(16):1311–18. doi:10.1182/blood.2019002766.

[2] Estrada-Veras JI, O'Brien KJ, Boyd LC, Dave RH, Durham B, Xi L, et al. The clinical spectrum of Erdheim-Chester disease: an observational cohort study. Blood Adv. 2017;1(6):357–66. doi:10.1182/bloodadvances.2016001784.

[3] Mazor RD, Manevich-Mazor M, Shoenfeld Y. Erdheim-Chester disease: a comprehensive review of the literature. Orphanet J Rare Dis 2013;8:137. doi:10.1186/1750-1172-8-137.

[4] Papo M, Emile JF, Maciel TT, Bay P, Baber A, Hermine O, et al. Erdheim-Chester disease: a concise review. Curr Rheumatol Rep 2019;21(12):66. doi:10.1007/s11926-019-0865-2.

[5] Goyal G, Heaney ML, Collin M, Cohen-Aubart F, Vaglio A, Durham BH, et al. Erdheim-Chester disease: consensus recommendations for evaluation, diagnosis, and treatment in the molecular era. Blood 2020;135(22):1929–45. doi:10.1182/blood.2019003507.

[6] Cives M, Simone V, Rizzo FM, Dicuonzo F, Cristallo Lacalamita M, et al. Erdheim-Chester disease: a systematic review. Crit Rev Oncol Hematol 2015;95(1):1–11. doi:10.1016/j.critrevonc.2015.02.004.

[7] Antunes C, Graça B, Donato P. Thoracic, abdominal and musculoskeletal involvement in Erdheim-Chester disease: CT, MR and PET imaging findings. Insights Imaging. 2014;5(4):473-82. doi: 10.1007/s13244-014-0331-7.

[8] Kumar P, Singh A, Gamanagatti S, Kumar S, Chandrashekhara SH. Imaging findings in Erdheim-Chester disease: what every radiologist needs to know. Pol J Radiol 2018;83:e54–62. doi:10.5114/pjr.2018.73290.

[9] Munoz J, Janku F, Cohen PR, Kurzrock R. Erdheim-Chester disease: characteristics and management. Mayo Clin Proc 2014;89(7):985–96. doi:10.1016/j.mayocp.2014.01.023.

[10] Starkebaum G, Hendrie P. Erdheim-Chester disease. Best Pract Res Clin Rheumatol 2020;34(4):101510. doi:10.1016/j.berh.2020.101510.

[11] Lozano JG, Lopez-Negrette L, Sanchez JL, Sala J. Erdheim-Chester disease. Eur J Radiol 1999;30(1):70–4. doi:10.1016/s0720-048x(98)00013-8.

[12] Arnaud L, Malek Z, Archambaud F, Kas A, Toledano D, Drier A, et al. 18F-fluorodeoxyglucose-positron emission tomography scanning is more useful in followup than in the initial assessment of patients with Erdheim-Chester disease. Arthritis Rheum 2009;60(10):3128–38. doi:10.1002/art.24848.

[13] Drier A, Haroche J, Savatovsky J, Godenèche G, Dormont D, Chiras J, et al. Cerebral, facial, and orbital involvement in Erdheim-Chester disease: CT and MR imaging findings. Radiology 2010;255(2):586–94. doi:10.1148/radiol.10090320.

[14] Arnaud L, Hervier B, Néel A, Hamidou MA, Kahn JE, Wechsler B, et al. CNS involvement and treatment with interferon-α are independent prognostic factors in Erdheim-Chester disease: a multicenter survival analysis of 53 patients. Blood 2011;117(10):2778–82. doi:10.1182/blood-2010-06-294108.

[15] Sedrak P, Ketonen L, Hou P, Guha-Thakurta N, Williams MD, Kurzrock R, et al. Erdheim-Chester disease of the central nervous system: new manifestations of a rare disease. AJNR Am J Neuroradiol 2011;32(11):2126–31. doi:10.3174/ajnr.A2707.

[16] Parks NE, Goyal G, Go RS, Mandrekar J, Tobin WO. Neuroradiologic manifestations of Erdheim-Chester disease. Neurol Clin Pract 2018;8(1):15–20. doi:10.1212/CPJ.0000000000000422.

[17] Lachenal F, Cotton F, Desmurs-Clavel H, Haroche J, Taillia H, Magy N, et al. Neurological manifestations and neuroradiological presentation of Erdheim-Chester disease: report of 6 cases and systematic review of the literature. J Neurol 2006;253(10):1267–77. doi:10.1007/s00415-006-0160-9.

[18] Merritt H, Pfeiffer ML, Richani K, Phillips ME. Erdheim-Chester disease with orbital involvement: case report and ophthalmic literature review. Orbit 2016;35(4):221–6. doi:10.1080/01676830.2016.1176211.

[19] Haroche J, Cluzel P, Toledano D, Montalescot G, Touitou D, Grenier PA, et al. Images in cardiovascular medicine. Cardiac involvement in Erdheim-Chester disease: magnetic resonance and computed tomographic scan imaging in a monocentric series of 37 patients. Circulation 2009;119(25):e597–8. doi:10.1161/CIRCULATIONAHA.108.825075.

[20] Cohen-Aubart F, Emile JF, Carrat F, Helias-Rodzewicz Z, Taly V, Charlotte F, et al. Phenotypes and survival in Erdheim-Chester disease: results from a 165-patient cohort. Am J Hematol 2018;93(5):E114–17. doi:10.1002/ajh.25055.
[21] Lodhi U, Sarmast U, Khan S, Yaddanapudi K. Multisystem radiologic manifestations of Erdheim-Chester disease. Case Rep Radiol. 2016;2016:2670495. doi:10.1155/2016/2670495.
[22] Haroche J, Amoura Z, Touraine P, Seilhean D, Graef C, Birmelé B, et al. Bilateral adrenal infiltration in Erdheim-Chester disease. Report of seven cases and literature review. J Clin Endocrinol Metab 2007;92(6):2007–12. doi:10.1210/jc.2006-2018.
[23] Arnaud L, Pierre I, Beigelman-Aubry C, Capron F, Brun AL, Rigolet A, et al. Pulmonary involvement in Erdheim-Chester disease: a single-center study of thirty-four patients and a review of the literature. Arthritis Rheum 2010;62(11):3504–12. doi:10.1002/art.27672.
[24] Diamond EL, Durham BH, Ulaner GA, Drill E, Buthorn J, Ki M, et al. Efficacy of MEK inhibition in patients with histiocytic neoplasms. Nature 2019;567(7749):521–4. doi:10.1038/s41586-019-1012-y.